Mater Renew Sustain Energy (2015) 4:19
DOI 10.1007/s40243-015-0062-9

ORIGINAL PAPER

Effect of transition metals on ball-milled $MmNi_5$ hydrogen storage alloy

Sumita Srivastava[1] · **Kuldeep Panwar**[1]

Received: 8 May 2015 / Accepted: 16 September 2015 / Published online: 30 September 2015

Abstract $MmNi_5$ hydrogen storage alloy has been ball-milled with transition metal Co/Ni/Mn/Fe, one at a time in small amount of 0.5, 1.0, 2.0 and 5.0 wt%. Optimum hydrogenation behaviour has been observed for the sample containing 2.0 wt% of transition metal. Maximum hydrogen storage capacities of the $MmNi_5$ alloy have been obtained as 1.68, 1.64, 1.56 and 1.52 wt%. Time taken for the maximum hydrogen absorption was recorded as 3.0, 4.0, 4.0 and 4.5 min and desorption took 1.9, 3.0, 3.5 and 4.0 min. Short-term cyclic performance has been improved as 98, 98, 97 and 96 % storage capacity retention after 20 cycles upon ball-milling with Co, Ni, Mn and Fe, respectively. The improvement in hydrogenation behaviour due to addition of transition metal has been obtained as Co > Ni > Mn > Fe. Structural and microstructural characterizations have been carried out by XRD and SEM techniques. Several factors have been discussed which affect catalytic action of transition metals in ball-milled $MmNi_5$ alloy.

Keywords $MmNi_5$ alloy · ball-milling · 3d-transition metal · Catalyst · XRD · SEM

Introduction

Key factor for the growth of hydrogen economy is development of an efficient hydrogen storage material. Being the safest hydrogen storage mode, metal hydride is very much attractive to the hydrogen researchers. Due to easy activation and ability to operate at ambient condition, $MmNi_5$ hydrogen storage alloy is important among metal hydrides [1–3]. However, higher pressure (>7 MPa) required for hydrogenation and low hydrogen storage capacity (1.4 wt%) decrease its popularity from application point of view.

Ball-milling of hydrogen storage alloy to obtain nanoparticle is already known to improve the hydrogenation behaviour of AB_5-type and other metal hydrides [4–7]. Nanocrystalline metal hydrides of Mg_2Ni, FeTi and $LaNi_5$ have shown enhanced absorption–desorption kinetics at lower temperature and pressure as compared to traditional hydrides [4]. Corre et al. found better discharge capacity of ball-milled $LaNi_5$ electrode in comparison to un-milled $LaNi_5$ electrode [5]. Ball-milling of magnesium hydride has modified the structure and increased the specific surface area [6]. Much faster sorption have been found for milled alloy as compared to un-milled one [6]. Annealing of mechanically alloyed $LaNi_5$ led to grain growth, release of microstrain and increase of storage capacity [7].

Nowadays many investigations have been performed on the effect of transition metal catalyst on Mg-based hydrogen storage alloys to further improve hydrogenation properties like hydrogen storage capacity, kinetics and dissociation temperature [8–15]. Mechanical milling of MgH_2 with 3d-transition metals showed different catalytic effect on reaction kinetics for different transition metal [8]. Most rapid absorption kinetics was noticed for Ti > V> Fe > Mn > Ni; while fastest desorption kinetics was observed for V > Ti > Fe > Ni > Mn [8]. Addition of Co during reactive mechanical alloying (RMA) has been found to increase the quantity of MgH_2 formed [9]. In a separate study during RMA of Mg with 3d-transition metal, Bobet et al. have found that hydriding resulted from the

✉ Sumita Srivastava
sumita_uki1@rediffmail.com

[1] Department of Physics, Government Post Graduate College, Rishikesh 249201, India

combination of two steps; nucleation at first and then diffusion [10]. A direct relationship was observed between the nucleation duration and the specific surface area by Bobet et al. [10]. Ershova et al. have shown in their study that addition of transition metals during RMA decreased the decomposition temperature of MgH_2 [11]. In one more report it was mentioned that transition metals enhanced the activation process during RMA of MgH_2 and activation was completed after two hydriding–dehydriding cycles [12]. A decrease in activation energy of MgH_2 as 45.67 kJ mol^{-1} as compared to 81.34 kJ mol^{-1} was noticed by Shahi et al., when nanocrystalline MgH_2 was co-catalysed with transition metals Ti, Fe and Ni [13]. According to Mamula et al., transition metals have different bonding with hydrogen atoms; thus weaken Mg–H bond and destabilized the surrounding MgH_2 matrix [14]. Jain et al. have reviewed Mg-based metal hydride and found that nanocomposites using various transition metal catalysts, alanates, nanocarbon, thin films, multilayered films, etc. may further improve the hydrogenation properties [15].

It was observed by Shan et al. that mechanical grinding of a small amount of Pd/Pt with AB_5-type intermetallic hydrogen storage alloys greatly improved the hydrogen absorption and desorption performances of the alloys [16]. The alloy retained both the low activation pressures and fast absorption–desorption rates even after more than 2 years of exposure in open air. According to Shan et al., enhanced hydrogen spillover and reverse hydrogen spillover were the primary processes that account for the improved hydrogen storage performance after Pd/Pt treatment [16].

Although transition metals have tendency to improve the hydrogenation properties, their catalytic effects on $MmNi_5$ hydrogen storage alloy have not been addressed in the literature till now. Present investigation is aimed to study the effect of transition metals (Co/Ni/Mn/Fe) on the hydrogenation behaviour of ball-milled $MmNi_5$ alloy.

Experimental details

Synthesis

As-received $MmNi_5$ alloy (Sigma-Aldrich) was ball-milled in self-constructed ball-mill. The atomic composition of mischmetal in $MmNi_5$ alloy was La—25 %, Ce—54 %, Pr—6 % and Nd—15 %. Ball-mill was carried out at 200 rpm for 3 h in a vial of 891 cc, taking 5 gm alloy at a time. During ball-milling, steel balls of diameter 1.22 cm and mass 10.5 gm were used. Ball to alloy powder weight ratio was kept at 100:1. Different grinding medium (dry/benzene/hexane/acetone) was selected for ball-milling of $MmNi_5$ alloy. For each grinding medium particle size distribution was recorded using sieves of different size. Figure 1 shows the particle size distribution after ball-milling. When acetone was used as grinding medium 65 % alloy had particle size less than 40 μm, which was the highest percentage yield of particles below 40 micron among all grinding media, hence acetone was used as grinding medium in all the experiments. Alloy samples have been prepared by ball-milling $MmNi_5$ hydrogen storage alloy together with high-purity (99.99 %) transition metals Co, Ni, Mn, and Fe taking one at a time. For each transition metal, four samples have been prepared by varying the concentration of transition metal with respect to $MmNi_5$ hydrogen storage alloy. The concentration of transition metal with respect to $MmNi_5$ hydrogen storage alloy has been kept at 0, 0.5, 1.0, 2.0 and 5.0 wt%. Initial size of $MmNi_5$ hydrogen storage alloy was 300 μm and transition metal catalyst was 40 μm.

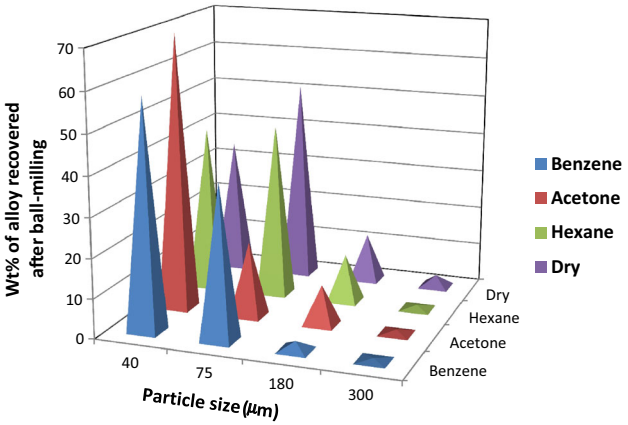

Fig. 1 Particle size distribution after ball-milling with different grinding medium

Structural and microstructural characterization

For structural characterization, all the ball-milled samples were subjected to X-ray diffraction (XRD) analysis to see the appearance of any new phase during ball-milling with transition metal. To depict the surface morphology and particle size distribution ball-milled and hydrogenated samples were microstructurally characterized by scanning electron microscope (SEM). XRD was done employing D8 ADVANCE BRUKER X-ray diffractometer that operated with copper K_α radiation. Microstructures were examined by means of a scanning electron microscope (SEM, LEO 435 VP) that employed a 30 kV secondary electron imaging mode.

Hydrogenation behaviour

Hydrogenation behaviour of all the samples was studied by monitoring pressure–composition isotherms, absorption–desorption kinetics and short-term cycling effect. The amount of hydrogen absorbed was monitored by measuring the decrease in hydrogen pressure of reactor, when it was closed. The decrease in hydrogen pressure was correlated to the volume of reactor to calculate the amount of hydrogen absorbed by the hydrogen storage alloy. The hydrogen desorbed was evaluated through water displacement method using Sievert's apparatus [17]. Between each hydrogenation–dehydrogenation cycle reactor was evacuated at a pressure of 10^{-11} MPa. Error in pressure measurement is 0.01 MPa, and in storage capacity it is 0.002 wt%. Time measurement has error of 0.1 min.

Results and discussions

Structural and microstructural characterization

All samples prepared by ball-milling of $MmNi_5$ alloy with transition metals are subjected to X-ray diffraction analysis for structural characterization. Figure 2 demonstrates a representative X-ray diffractogram of $MmNi_5$ alloy ball-milled with transition metal Co/Ni/Mn/Fe having concentration of 2.0 wt%. In all XRD patterns, $CaCu_5$-type structure for $MmNi_5$ alloy is depicted. After ball-milling of $MmNi_5$ alloy with transition metal no new phases are detected. Lattice parameters and unit cell volume of all the samples are given in Table 1. No remarkable change is observed in lattice parameters after ball-milling with transition metal. This suggests that during the process of ball-milling transition metal has not dissolved into $MmNi_5$ alloy; rather they are physically mixed with the alloy during ball-milling. Thus, transition metal particles may be at the surface of the particles of hydrogen storage alloy. Since the amount of transition metal is small during ball-milling, no peaks of transition metals are observed at concentration of 0–2.0 wt%. However, small XRD peaks of transition metals are detected at concentration of 5.0 wt%.

XRD pattern corresponding to bulk $MmNi_5$ alloy shows less broadening in the XRD peaks, exhibiting large crystallite size (40 nm). In all the other XRD patterns corresponding to ball-milled $MmNi_5$ alloy with or without transition metal almost equal peak broadening can be seen. The average crystallite size of all the ball-milled samples, calculated through XRD peak broadening employing Scherrer equation is found to lie within the range of 15–20 nm as given in Table 1.

To see the surface morphology and particle size distribution after ball-milling, the samples are microstructurally

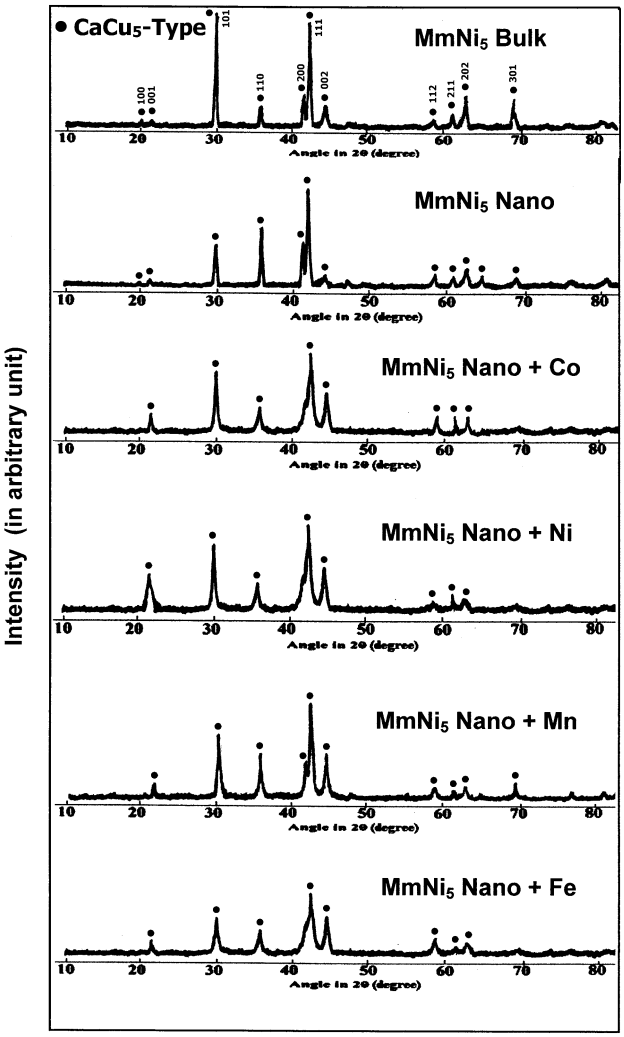

Fig. 2 XRD patterns of $MmNi_5$ alloy ball-milled with transition metals at concentration of 2.0 wt%

characterized by scanning electron microscopy. Figure 3a–f represents scanning electron micrographs of as-received $MmNi_5$ alloy and ball-milled with transition metal at concentration of 2.0 wt%. Figure 3a representing SEM photograph of as-received bulk $MmNi_5$ alloy, exhibits inhomogeneous particle size distribution ranging from 5 to 50 μm. Fractures in the big particles can be seen in ball-milled $MmNi_5$ alloy (Fig. 3b). SEM micrograph (Fig. 3c) of $MmNi_5$ alloy ball-milled with Co reveals a homogeneous distribution of particles of the size 2 μm. Comparatively smaller particles are depicted in SEM micrograph (Fig. 3d) of alloy ball-milled with Ni. When Mn is used during ball-milling an inhomogeneous distribution of particles of the size lying within range of 1–2 μm (Fig. 3e) can be seen. Similar micrograph is obtained for transition metal Fe (Fig. 3f). Hence, when Co is used during ball-milling, most homogeneous microstructure is obtained. Hardness and elasticity of the added transition metal during ball-

Table 1 Lattice parameters, unit cell volume and average crystallite size of $MmNi_5$ alloy, ball-milled with transition metal at the concentration of 2.0 wt%

S.n.	Name of the sample	Lattice parameter 'a' (Å)	Lattice Parameter 'c' (Å)	Unit cell volume (Å^3)	Average crystallite size (nm)
1	$MmNi_5$ Bulk	4.9793	4.0701	87.3896	40
2	$MmNi_5$ Nano	4.9915	4.0649	87.7061	20
3	$MmNi_5$ Nano + Co	4.9916	4.0652	87.7161	18
4	$MmNi_5$ Nano + Ni	4.9912	4.0650	87.6977	17
5	$MmNi_5$ Nano + Mn	4.9915	4.0653	87.7148	15
6	$MmNi_5$ Nano + Fe	4.9917	4.0652	87.7196	16

milling may affect the resultant microstructure. Hard transition metal particles added during milling will act like balls and will help in grinding the hydrogen storage alloy. Less elasticity of the added transition metal will help in preserving its own shape and size up to some extent during ball-milling and hence transition metal particles will disperse homogeneously on the surface of the alloy particles. Brinell hardness of Co, Ni, Fe and Mn is 470–3000, 667–1600, 200–1180 and 196 MPa, respectively [18]. Similarly bulk modulus of Co, Ni, Fe and Mn are 180, 180, 170 and 120 GPa [18]. Hence, Co is the hardest and least elastic transition metal among the selected group. The combined effect of hardness and elasticity may be responsible for the homogeneous microstructure of the $MmNi_5$ alloy ball-milled with Co.

Figure 4a–f represents SEM micrographs of ball-milled $MmNi_5$ alloy taken after 20 hydrogenation–dehydrogenation cycles excluding activation cycles. As revealed by these micrographs particle size reduces from initial size to smaller size. Bulk alloy is found to change in a powder of the size 5–10 μm after 20 hydrogenation–dehydrogenation cycles (Fig. 4a). Again an inhomogeneous reduction in particle size (1–3 μm) is noted in Fig. 4b corresponding to $MmNi_5$ alloy ball-milled without transition metal. A homogeneous morphology is depicted in the alloy ball-milled with Co transition metal. In this case, particles change into size of 1 μm (Fig. 4c). Similar pattern of microstructure with inhomogeneous particle size reduction ranging from 0.5 to 2 μm can be seen in Fig. 4d corresponding to alloy ball-milled with Ni. Even more reduction in particle size (<1 μm) is noted in the case of Mn and Fe (Fig. 4e, f); however, when Fe is used comparatively larger particles are depicted than Mn. The reduction in particle size in all the samples is due to volume expansion during hydrogenation–dehydrogenation cycles known as pulverization. Again, the alloy ball-milled with Co transition metal gives optimum microstructure after 20 hydrogenation–dehydrogenation cycles. It has been reported by Sarma et al. that an optimum particle size is needed for obtaining best hydrogenation properties [2].

Hydrogenation behaviour

In present investigation, six types of sample are studied for their hydrogenation behaviour. Except the bulk $MmNi_5$ alloy, other samples are found to absorb hydrogen in the first cycle. In case of the bulk alloy it takes five cycles to activate completely. The fast activation in the ball-milled samples is due to the small size of particles (2–5 μm) and nanosize of the crystallites. During the process of ball-milling the surface area and grain boundary increases which provides channel to hydrogen for absorption and desorption process. Hydrogenation behaviour is monitored by varying the concentration of added transition element as $x = 0$, 0.5, 1.0, 2.0 and 5.0 wt%. Optimum hydrogenation behaviour is obtained at the concentration of 2.0 wt%.

Absorption p–c isotherms for all the six samples have been plotted in Fig. 5. Every curve has clear cut plateau region. The slope of the plateau increases after ball-milling. During the process of ball-milling, particle and crystallite size reduces, resulting in an increase of grain boundary, which works like amorphous region, imparting slope to p–c isotherm [7]. Ball-milling reduces the absorption plateau pressure from 7 to 4.7 MPa. The plateau pressure is calculated at half of the maximum storage capacity. Absorption–desorption plateau pressure of all $MmNi_5$ alloy ball-milled with transition metals at concentration $x = 2.0$ wt% is given in Table 2. The effect of transition metal catalyst in lowering the plateau pressure is in order of Ni > Co > Fe > Mn. Figure 6 represents desorption p–c isotherms of all the samples. Desorption plateau pressure also reduces due to addition of transition element (Table 2). Reduction in absorption–desorption plateau pressure indicates that addition of transition element lowers the driving force. The reduction in driving force may be due to catalytic action of transition metals to dissociate hydrogen molecule into hydrogen atoms, which are diffused in metal hydride through channels provided by grain boundaries in nanomaterial [19]. The amount of added transition metal affects the hydrogen storage capacity. The storage capacity increases with increase in amount of

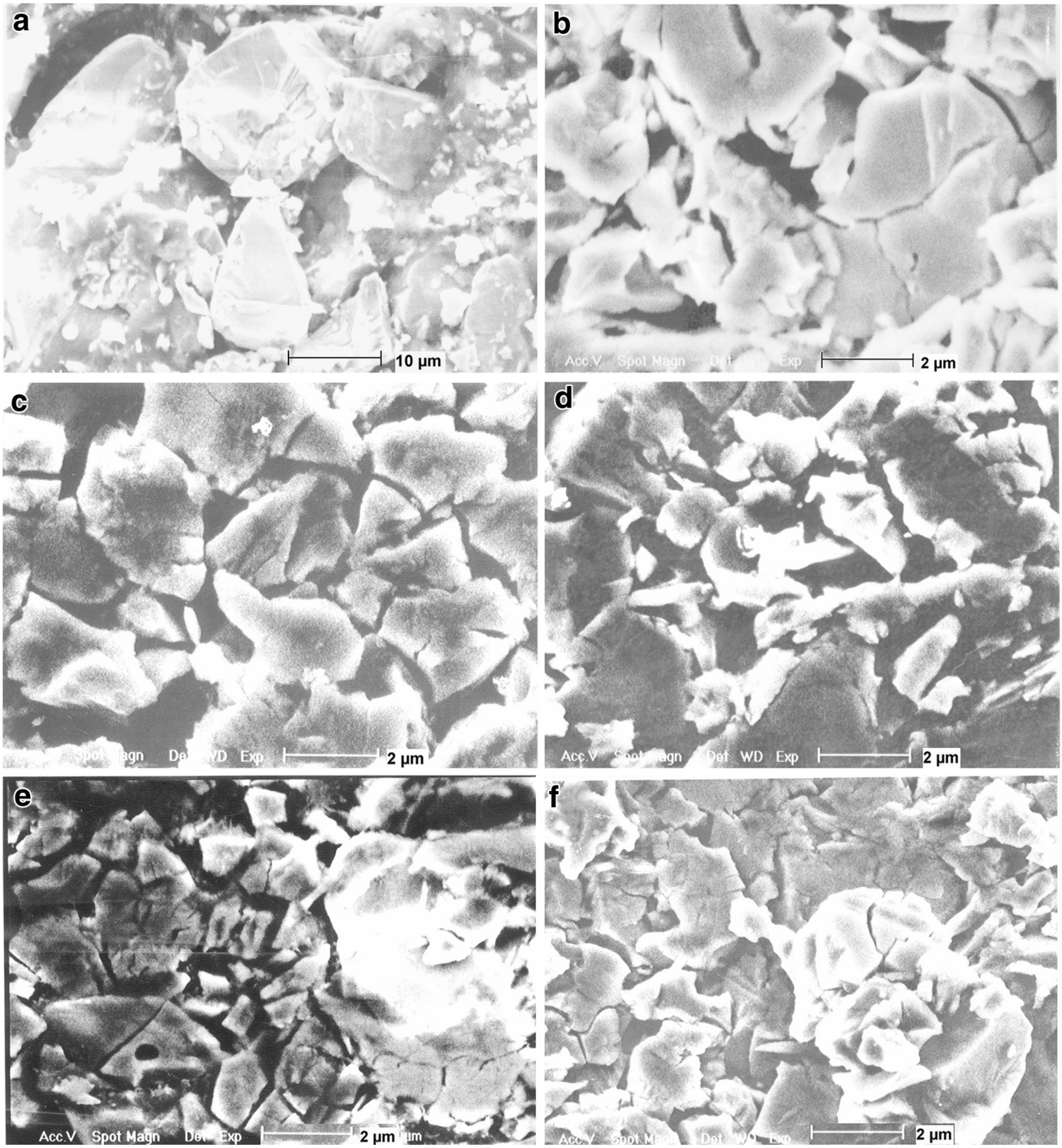

Fig. 3 SEM micrographs of **a** bulk $MmNi_5$ alloy, **b** ball-milled $MmNi_5$ alloy, **c** $MmNi_5$ alloy ball-milled with Co, **d** Ni, **e** Mn and **f** Fe transition metals at concentration of 2.0 wt%

transition metal from $x = 0$ to $x = 2.0$ wt%. After attaining maximum capacity at $x = 2.0$, it again reduces at $x = 5.0$ wt%. Maximum hydrogen storage capacities of the $MmNi_5$ alloy have been obtained as 1.68, 1.64, 1.56 and 1.52 wt% on ball-milling with Co, Ni, Mn and Fe, respectively, at the concentration of 2.0 wt%. Table 3 shows hydrogen storage capacity of ball-milled $MmNi_5$ with different concentration (x) of transition metal. Very small amount of added transition metal may not provide the required catalytic action. Since transition metal itself does not absorb hydrogen reversibly like $MmNi_5$, higher concentration of transition metal reduces the overall hydrogen storage capacity. Similar result has been obtained by Shahi et al., where authors have studied nanocrystalline MgH_2

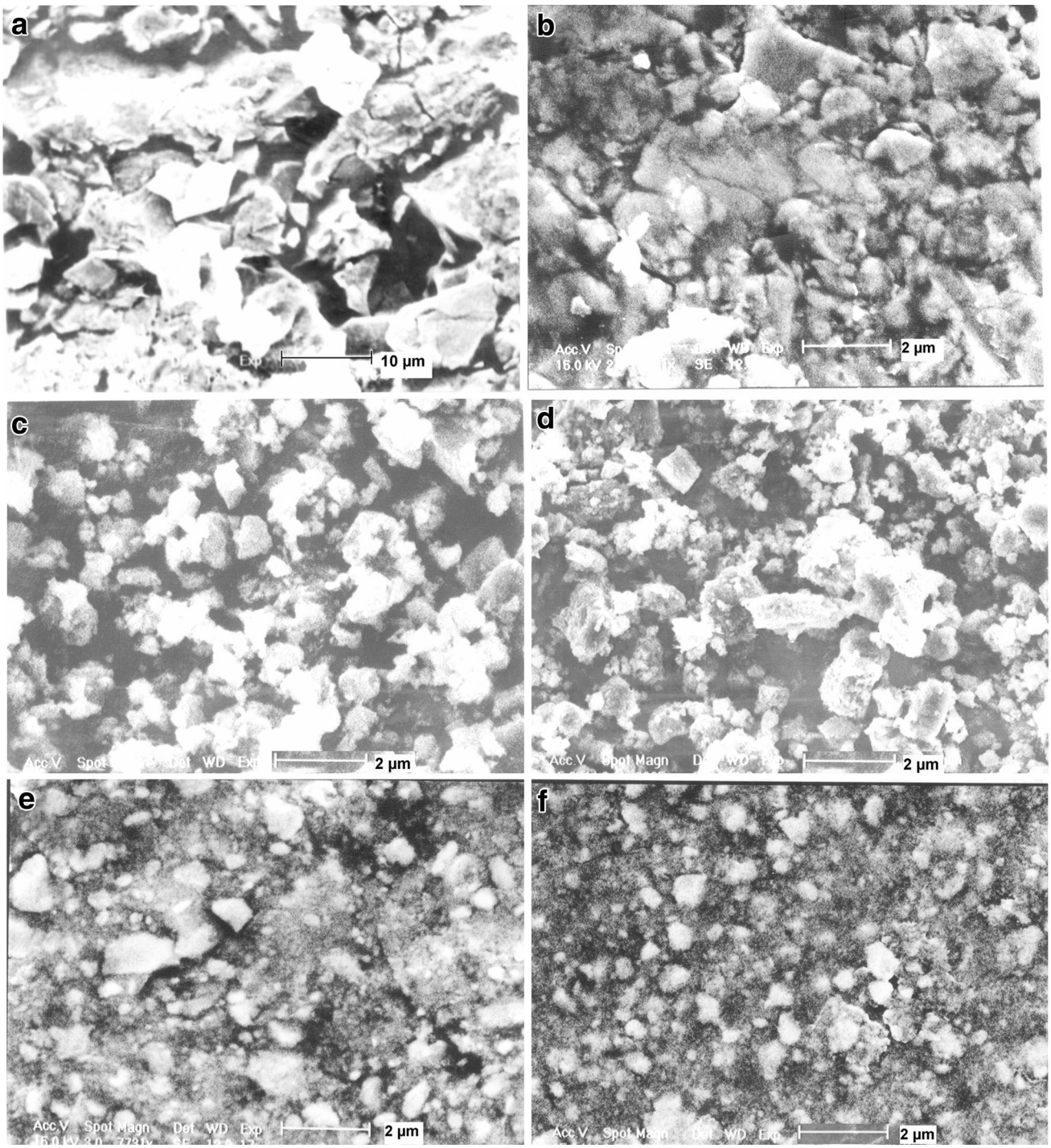

Fig. 4 SEM micrographs of hydrogenated/dehydrogenated **a** bulk $MmNi_5$ alloy, **b** ball-milled $MmNi_5$ alloy, **c** $MmNi_5$ alloy ball-milled with Co, **d** Ni, **e** Mn and **f** Fe transition metals at concentration of 2.0 wt%

co-catalysed with Ti, Fe and Ni [13]. They have reported optimum capacity at 5 wt%, which reduces after increasing the concentration of transition metals.

In the present investigation, maximum hydrogen storage capacity is found as 1.68 wt%, when 2.0 wt% Co is added during ball-milling of $MmNi_5$ alloy. This higher capacity is thought to be due to addition of transition metal. Earlier study suggests that presence of catalyst during ball-milling may enhance the kinetic reaction [8]. In the present case, it appears that catalyst also affects the storage capacity. Although transition metal itself does not store hydrogen reversibly, its catalytic action in transferring hydrogen

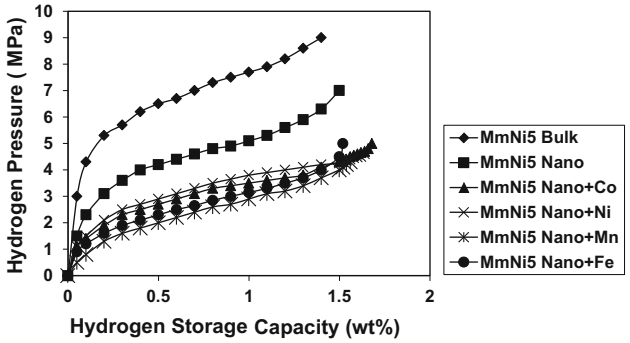

Fig. 5 Absorption p–c isotherms of $MmNi_5$ alloy ball-milled with transition metals at concentration of 2.0 wt%

Table 2 Absorption–desorption plateau pressure of $MmNi_5$ alloy ball-milled with transition metals at concentration $x = 2.0$ wt%, calculated at half of the maximum storage capacity of p–c isotherm

Alloy specification	Absorption plateau pressure (MPa)	Desorption plateau pressure (MPa)
$MmNi_5$ Bulk	7.00	1.20
$MmNi_5$ Nano	4.70	1.50
$MmNi_5$ Nano + Co	3.35	0.87
$MmNi_5$ Nano + Ni	3.52	0.68
$MmNi_5$ Nano + Mn	2.58	0.98
$MmNi_5$ Nano + Fe	2.75	1.08

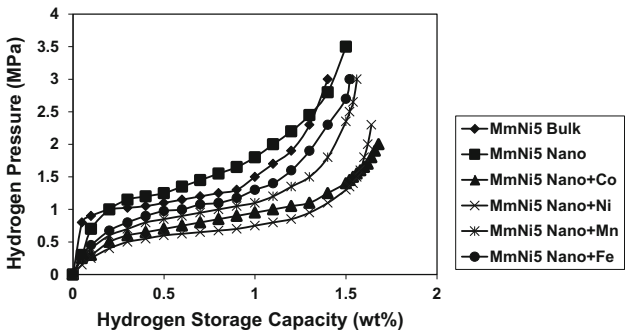

Fig. 6 Desorption p–c isotherms of $MmNi_5$ alloy ball-milled with transition metals at concentration of 2.0 wt%

atoms at suitable sites in metal hydride matrix may be responsible for increased hydrogen storage capacity in nanocrystalline $MmNi_5$ alloy, when ball-milled with transition metal. There are many factors which affect the catalytic action of transition metals. These are listed in the end of this section. The factor, which affects the storage capacity, is electronegativity difference between transition metal and the alloy. In metal hydride (MH) matrix M is electropositive and H is electronegative. First of all hydrogen molecule is dissociated into hydrogen atoms at the surface of transition metal particle and further hydrogen may be stored as ion in the MH matrix. The more electronegativity of transition metal will repel H^- ion and force the ion to go towards M^+ ion. The larger be the difference between electronegativity of M and transition metal, the more guided path will be followed by H^- ion. The electronegativity factor of Ce and La in $MmNi_5$ is 1.12, while for Co, Ni, Mn and Fe it is 1.88, 1.91, 1.55 and 1.83. The maximum difference of electronegativity factor between M and transition metal is for Ni and Co. It is noteworthy that this factor will not create extra vacancies for hydrogen, but it will force the hydrogen ion to take over all the vacancies created by any means. Enhancement in storage capacity is not only due to this factor. The higher capacity may be due to the combined effect of catalytic action of added transition metal and optimum microstructure produced during ball-milling in the presence of transition metal. It may be mentioned here that earlier study on ball-milled $MmNi_{4.6}Fe_{0.4}$ alloy showed storage capacity of 1.7 wt% [2]. Hence, the higher capacity in the present case appears reliable. According to Ershova et al., the reason behind increased storage capacity in nanocrystalline hydrogen storage alloy, may be due to storage of hydrogen at another location in ball-milled alloy [20]. Creation of high density of defects, grains and sub-grain boundaries and other imperfections of crystal lattice during ball-milling may act as stable sites for hydrogen storage together with regular positions in crystal lattice. The interface between hydrogen storage alloy and catalyst acts as an active nucleation site for the hydride phase [21]. 3d-transition metal reduces the nucleation barrier. Hence, incorporation of transition metal catalyst,

Table 3 Hydrogen storage capacity of $MmNi_5$ alloy ball-milled at various concentrations (x) of transition metals

Hydrogen storage capacity (wt%) at concentration x (wt%)					
Alloy specification	$x = 0$	$x = 0.5$	$x = 1.0$	$x = 2.0$	$x = 5.0$
$MmNi_5$ Bulk	1.40	–	–	–	–
$MmNi_5$ Nano	1.50	–	–	–	–
$MmNi_5$ Nano + Co	1.50	1.56	1.60	1.68	1.61
$MmNi_5$ Nano + Ni	1.50	1.54	1.58	1.64	1.58
$MmNi_5$ Nano + Mn	1.50	1.52	1.54	1.56	1.52
$MmNi_5$ Nano + Fe	1.50	1.50	1.52	1.52	1.48

during ball-milling in creating nanocrystalline version of hydrogen storage alloy gives synergetic effect to improvement of hydrogenation characteristics. One more reason for higher storage capacity may be elasticity of MH matrix. According to Pasquini et al., volume expansion in the lattice due to storage of hydrogen atom at interstitial position favours the absorption of further H atoms resulting in net H–H attraction [22]. However, if lattice is not free to expand upon H absorption, the H–H interaction might even turn into a repulsive one. In nanocrystalline material, at the interface of catalyst and MH matrix elasticity is comparatively large.

Absorption and desorption kinetic curves of ball-milled $MmNi_5$ alloy with 2.0 wt% transition metal are given in Figs. 7 and 8, respectively. Whereas, bulk $MmNi_5$ alloy takes more than 5 min to absorb maximum amount of hydrogen, its nanoversion takes about 5 min to complete the process. Addition of transition metal during ball-milling further increases the absorption kinetics. Time taken to absorb the maximum amount of hydrogen on addition of Co, Ni, Mn and Fe corresponds to 3.0, 4.0, 4.0 and 4.5 min, respectively. Similar characteristics are noted in case of the desorption kinetics. During desorption it takes 1.9, 3.0, 3.5 and 4.0 min to desorb 100 % hydrogen corresponding to transition element Co, Ni, Mn and Fe, respectively. Kinetic curves shown in Figs. 7 and 8 clearly indicate that absorption and desorption kinetic increases after ball-milling the $MmNi_5$ alloy. It further increases on adding transition metal during ball-milling due to catalytic action of transition metal. Absorption kinetics was monitored at maximum hydrogen pressure shown in p–c isotherm of respective sample in Fig. 5. Hence, for bulk alloy pressure was 90 Mpa, for ball-milled alloy it was 70 MPa and for transition metals, pressure was 40 MPa. All the desorption kinetics was monitored at 0.1 MPa.

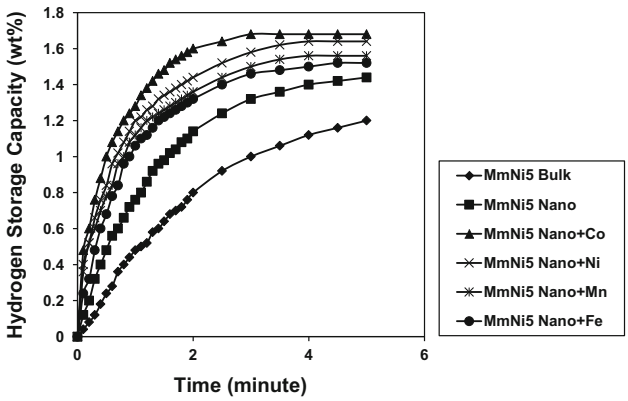

Fig. 7 Absorption kinetic curves of $MmNi_5$ alloy ball-milled with transition metals at concentration of 2.0 wt%

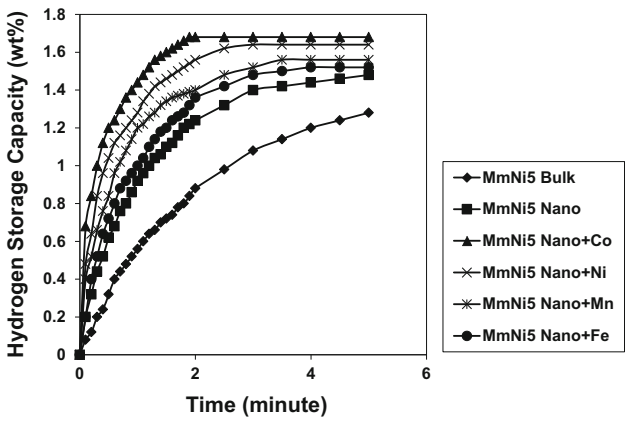

Fig. 8 Desorption kinetic curves of $MmNi_5$ alloy ball-milled with transition metals at concentration of 2.0 wt%

Short-term cyclic performance of ball-milled $MmNi_5$ alloy having 2.0 wt% of transition metal is illustrated in Fig. 9. This figure clearly indicates that addition of transition metal improves the decay in storage capacity due to repeated hydrogenation–dehydrogenation cycles. Addition of transition metal improves the retention of storage capacity after 20 cycles from 90 to 98 %, 98, 97 and 96 % corresponding to Co, Ni, Mn and Fe, respectively.

Although no work has been reported till now on the catalytic effect of transition metals on AB_5-type hydrogen storage alloy, similar results have been found in studies of the effect of transition metals on MgH_2 system. It has been shown that addition of transition metals during ball-milling of MgH_2 reduces the activation energy, thus improves absorption–desorption kinetics very much [8, 13]. Co has been found to be most effective in formation of large amount of MgH_2 [9]. According to Liang et al., transition metals are good catalyst for chemisorptions of hydrogen. They reduce the nucleation barrier and thus enhance the kinetics [8].

In present case also, Co has been found to be most effective in improving the hydrogenation behaviour like storage capacity, kinetics and cyclic stability. The

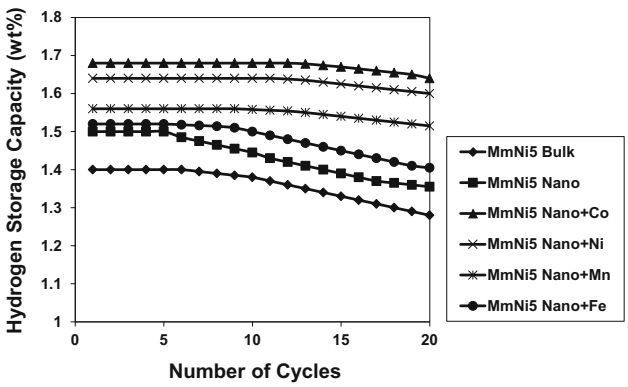

Fig. 9 Short-term cyclic performance of $MmNi_5$ alloy ball-milled with transition metals at concentration of 2.0 wt%

improvement in hydrogenation properties of $MmNi_5$ alloy by adding transition metal during ball-milling is in order of Co > Ni > Mn > Fe. This enhancement is due to catalytic action of transition metal. The order of transition metal in improving the hydrogenation properties is due to combined effect of their electronegativity, hardness and elasticity factors. There is not much difference between Mn and Fe; but the susceptibility of Fe to form oxide, decreases its ability over Mn.

There are many factors, which may affect the catalytic action of transition metals in ball-milled $MmNi_5$ alloy. These are listed in the following:

i. variable valency of catalyst
ii. size of catalyst
iii. defects introduced to the catalyst during ball-milling
iv. defects introduced in hydrogen storage alloys during ball-milling
v. spill over effect
vi. hardness of catalyst
vii. ability of catalyst to transfer stable diatomic hydrogen into the desired ionic configuration
viii. electron distribution and orbital structure
ix. lowering of activation energy due to catalyst
x. number of free electrons in the catalyst.

The study on the correlation of these factors with hydrogenation properties is on the way and will be communicated soon.

Conclusions

The overall hydrogenation behaviour of $MmNi_5$ alloy ball-milled with transition metal (Co/Ni/Mn/Fe) is improved. The improvement in hydrogen storage capacity, absorption–desorption kinetics, and short-term cyclic performance is thought to be due to catalytic action of added transition metal. Optimum results are obtained when transition metal is added at the concentration of 2.0 wt%. The improvement due to added transition metal is seen in the order of Co > Ni > Mn > Fe.

Acknowledgments Authors are grateful to Prof. O.N. Srivastava (BHU, INDIA) and Prof. I.P.Jain (Rajasthan University, INDIA) for helpful discussions. The financial support by University Grants Commission, New Delhi, India is gratefully acknowledged.

References

1. Barbir, F., Veziroglu, T.N., Plass Jr, H.J.: Environmental damage due to fossil fuels use. Int. J. Hydrogen Energy **15**, 739–749 (1990)
2. Sarma, V.V., Raman, S.S.S., Davidson, D.J., Srivastava, O.N.: On the mechanically pulverized $MmNi_{4.6}Fe_{0.4}$ as a viable hydrogen storage material. Int. J. Hydrogen Energy **26**, 231–236 (2001)
3. Sharma, V.K., Kumar, E.A.: Effect of measurement parameters on thermodynamic properties of La-based metal hydrides. Int. J. Hydrogen Energy **39**, 5888–5898 (2014)
4. Zaluski, L., Zaluska, A., Strom-Olsen, J.O.: Nanocrystalline metal hydrides. J. Alloys Compd. **253–254**, 70–79 (1997)
5. Corre, S., Bououdina, M., Kuriyama, N., Fruchart, D., Adachi, G.Y.: Effects of mechanical grinding on the hydrogen storage and electrochemical properties of $LaNi_5$. J. Alloys Compd. **292**, 166–173 (1999)
6. Huot, J., Liang, G., Boily, S., Neste, A.V., Schulz, R.: Structural study and hydrogen sorption kinetics of ball-milled magnesium hydride. J. Alloys Compd. **293–295**, 495–500 (1999)
7. Liang, G., Huo, T.J., Schulz, R.: Hydrogen storage properties of the mechanically alloyed $LaNi_5$-based materials. J. Alloys Compd. **320**, 133–139 (2001)
8. Liang, G., Huot, J., Boily, S., Neste, A.V., Schulz, R.: Catalytic effect of transition metals on hydrogen sorption in nanocrystalline ball-milled MgH_2-Tm (Tm = Ti, V, Mn, Fe and Ni) systems. J. Alloys Compd. **292**, 247–252 (1999)
9. Bobet, J.L., Even, C., Nakamura, Y., Akiba, E., Darriet, B.: Synthesis of magnesium and titanium hydride via reactive mechanical alloying influence of 3d-metal addition on MgH_2 synthesize. J. Alloys Compd. **298**, 279–284 (2000)
10. Bobet, J.L., Akiba, E., Nakamura, Y., Darriet, B.: Study of Mg-M (M=Co, Ni and Fe) mixture elaborated by reactive mechanical alloying-hydrogen sorption properties. Int. J. Hydrogen Energy **25**, 987–996 (2000)
11. Ershova, O.G., Dobrovolsky, V.D., Solonin, Y.M., Khyzhun, O.Y., Koval, A.Y.: Influence of Ti, Mn, Fe and Ni addition upon thermal stability and decomposition temperature of the MgH_2 phase of alloys synthesized by reactive mechanical alloying. J. Alloys Compd. **464**, 212–218 (2008)
12. Kwon, S.N., Baek, S.H., Mumm, D.R., Hong, S.H., Song, M.Y.: Enhancement of the hydrogen storage characteristics of Mg by reactive mechanical grinding with Ni, Fe and Ti. Int. J. Hydrogen Energy **33**, 4586–4592 (2008)
13. Shahi, R.R., Tiwari, A.P., Shaz, M.A., Srivastava, O.N.: Studies on de/rehydrogenation characteristics of nanocrystalline MgH_2 co-catalyzed with Ti, Fe, Ni. Int. J. Hydrogen Energy **38**, 2778–2784 (2013)
14. Mamula, B.P., Novakovic, J.G., Radisavjevic, I., Ivanovic, N., Novakovic, N.: Electronic structure and charge distribution topology of MgH_2 doped with 3d transition metals. Int. J. Hydrogen Energy **39**, 5874–5887 (2014)
15. Jain, I.P., Lal, C., Jain, A.: Hydrogen storage in Mg: a most promising material. Int. J. Hydrogen Energy **35**, 5133–5144 (2010)
16. Shan, X., Payer, J.H., Jennings, W.D.: Mechanism of increased performance and durability of Pd-treated metal hydriding alloys. Int. J. Hydrogen Energy **34**, 363–369 (2009)
17. Ramakrishna, K., Singh, S.K., Singh, A.K., Srivastava, O.N.: Solid state materials for hydrogen storage. In: Dahiya, R.P. (ed.) Progress in Hydrogen Energy, vol. 7, pp. 81–110. Boston, Riedel (1987)

18. Samsonov, G.V. (ed.): Mechanical properties of the elements. handbook of the physicochemical properties of the elements. IFI-Plenum, New York (1968)
19. Pozzo, M., Alfe, D.: Hydrogen dissociation and diffusion on transition metal (=Ti, Zr, V, Fe, Ru Co, Rh, Ni, Pd, Cu, Ag): doped Mg (0001) surfaces. Int. J. Hydrogen Energy **34**, 1922–1930 (2009)
20. Ershova, O.G., Dobrovolsky, V.D., Solonin, YuM, Khyzhun, OYu., Koval, AYu.: Influence of Ti, Mn, Fe and Ni addition upon thermal stability and decomposition temperature of the MgH_2 phase of alloys synthesized by reactive mechanical alloying. J. Alloys Compds. **464**, 212–218 (2008)
21. Liang, G., Huot, J., Boily, S., Neste, A.Van, Schulz, R.: Catalytic effect of transition metals on hydrogen sorption in nanocrystalline ball-milled MgH_2-Tm (Tm=Ti, V, Mn, Fe and Ni) systems. J. Alloys Compds. **292**, 247–252 (1999)
22. Pasquini, L., Sacchi, M., Brighi, M., Boelsma, C., Bals, S., Perkisas, T., Dam, B.: Hydride destabilization in core-shell nanoparticles. Int. J. Hydrogen Energy **39**, 2115–2123 (2014)